DEVELOPMENT OF MATERIAL REMOVAL FUNCTION IN ATMOSPHERIC PRESSURE PLASMA JET MACHINING PROCESSING

Y. F. Zhang[1,2] – B. Wang[1*] – H. L. Jin[1] – S. Dong[1]

[1]Center for Precision Engineering, Harbin Institute of Technology, Harbin, 15001, China
[2]College of Mechatronic Engineering, Shenyang Aerospace University, Shenyang, 110136, China

ARTICLE INFO

***Article history*:**
Received: 15.3.2013.
Received in revised form: 8.5.2013.
Accepted: 13.5.2013.

Keywords:
Atmospheric pressure plasma
Atomic emission spectroscopy
Removal function model
Curve fit

Abstract:

The removal function is one of the key factors in achieving ultra-precision machining results by computer controlled optic surface principle. In the atmospheric pressure plasma jet machining process, the distribution of active radicals on the workpiece surface is one of the major factors that affect the removal function. However, the distribution of jet pressure on the workpiece surface affects the distribution of active radicals. The pressure distribution of the plasma jet effluent on the workpiece surface has been simulated according to jet theory. The spatial density distribution of active radicals is measured with atomic emission spectroscopy. The results show that there is a relationship between the active radical distribution and the jet pressure distribution. Finally, based on experimental data, the material removal function model has been developed by curve fitting, and in this model, the reactive gas flux and the distance between the nozzle and the workpiece is defined / calculated / obtained by the parameters of the removal function.

List of symbols

P - gas pressure, Pascal
V - gas volume, m^3
n - amount of substance, mol
R - ideal gas constant, J/(mol.K)
T - temperature, K
Lr - the flux of SF_6, SLM
D - machining distance, mm
a - parameter of gauss curve, mm
c - parameter of gauss curve, mm^2
P_{a1}~P_{a10} - fitting coefficient for parameter a
P_{c1}~P_{c10} - fitting coefficient for parameter c

1 Introduction

With the rapid development of micro-electronic technology and optical technology, applications of high precision and undamaged free form surface become increasingly widespread [1], and thus make the quality requirements of the surface more sophisticated. Especially for the processing of optical components of hard and brittle material (such as SiO_2, SiC, and WC), typical processes generally applied are still lowly efficient diamond-based cutting, grinding and various mechanical

* Corresponding author. Tel.: +86 451 8641 2534; fax: +86 451 8641 2534
E-mail address: bradywang@hit.edu.cn.

machining methods. As a result of contact machining, sub-surface damage of the material will inevitably occur, and it will affect the performance of optical components [2-3].

These problems can be solved efficiently by the atmospheric pressure plasma machining process. In the machining process, active species with high density are provided by plasma, and the removal of materials will be achieved by the chemical reaction between these active species and the surface of the workpiece. As a kind of a non-contact process, atmospheric plasma machining has lots of advantages such as high efficiency, high machining accuracy, freedom from defects on the surface, etc. Much effort has been devoted to research by Osaka University and Lawrence Livemore Laboratory, and it has resulted in a lot of applications [4-8]. Also, research into SiC substrates machining was carried out by the Center of Precession Engineer of the Harbin Institute of technology with the plasma device created by its own magnetic field [9].

The machining process is similar to the computer controlled optic surface (CCOS) process that uses atmospheric pressure plasma to manufacture an optic free surface. The amount of material removed is a convolution of the material removal function and dwell time during the atmospheric pressure machining process. The material removal function presents the ability to remove material and to profile after machining. Therefore, it is a key factor for machining accuracy and efficiency. Until now, the present documents have not offered a deep research report about the removal function of the atmospheric pressure plasma machining process. In this paper, however, the pressure of the plasma jet effluent attached to the workpiece is simulated according to the jet theory, and subsequently the relationship of material removal function and the pressure attached to the workpiece is derived from the simulation result. The spatial density distribution of active radicals is measured with the atomic emission spectroscopy and the relationship between processing velocity and the density distribution of active species is analyzed using experimental results. Finally, based on experiment data, the material removal function has been developed by the curve fitting method.

2 Mechanism of the material removal during atmospheric pressure plasma jet machining

Fig. 1 shows the schematic diagram of the plasma machining system used in this study. The inert gas Helium and the active gas SF_6 is fed from the inlet. The plasma is excited in the exciting area, and then the effluent is spurted from the outlet and delivered to the workpiece surface as plasma jet. The material is removed from the workpiece surface due to the chemical reaction between the active species and the material on the workpiece surface.

When the workpiece material is SiO_2, the chemical reaction that might occur is shown in Equation (1) and (2).

$$SiO_2+xF^*(g)=SiFx(g)+O_2(g) \quad (1)$$

$$S(g)+2O(g)=SO_2(g) \quad (2)$$

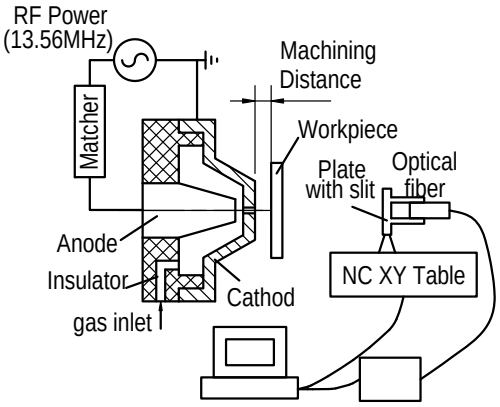

Figure 1. Schematic diagram of the machining system.

According to the theory of chemical reactive dynamics, the chemical reactive velocity is determined by the reactant concentration. That means that the active fluorine atomics concentration affects the reactive velocity during atmospheric pressure plasma machining. More material is removed where the active fluorine atomic concentration is higher where the machining profile is deeper. However, according to the ideal gas state equation, shown in Equation (3), the active fluorine atomic amount n is proportional to the gas pressure P under the same condition, that is, $n \propto P$. So, the pressure distribution and the spatial distribution of the active species on the workpiece surface are two key factors of the footprint of the removal function.

$$PV = nRT \quad (3)$$

3 Analysis of the influent factors for the removal function

3.1 Plasma jet pressure distribution analysis on the workpiece surface

Solving the velocity and pressure distribution of the plasma jet effused from the plasma torch nozzle is a typical two-dimensional axisymmetric problem. To simplify the problem, the plasma jet is assumed to be a type of liquid/fluid flow with constant, ax-symmetric, inviscid, adiabatic characteristics. Furthermore, there is no participation of the volume force and chemical reactions. That means that the fluid in a flow field takes on the same physical characteristics.

The pressure distribution of plasma jet is simulated with ANSYS software according to jet theory and the result is shown in Fig. 2. This figure shows that the axial pressure of plasma jet decreases rapidly away from the jet center on the workpiece surface and that the maximum pressure is at the center of the impact point. The profile of pressure distribution is a Gauss curve line. The pressure distribution by simulation is the same as the fluid pressure distribution of the workpiece surface by the theory of the wall jet given by Glauert [10].

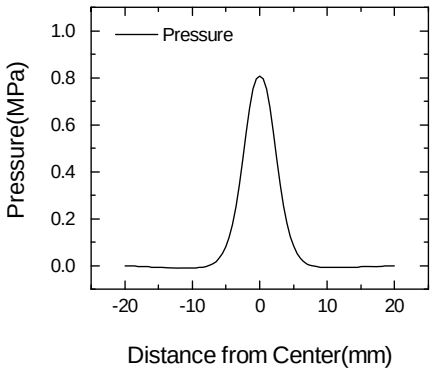

Figure 2. Pressure distribution on workpiece surface.

3.2 Distribution of the active species density in the atmospheric pressure plasma

The intensity of the active radicals was measured with atomic emission spectrometry [11] and used as a basis for the density determination. Table 1 shows the experimental parameters.

Table 1. Experiment parameters

He Flux	SF_6 Flux	Supplied Power	Machining Distance
SLM	SLM	w	mm
1	0.06	200	6

The plasma is excited by the mixture of exciting gas (He) and reactive gas (SF_6), which includes active F* radical that is required in the chemical reaction during machining. The density curve along the radial direction is obtained by measuring the intensity of F* atomic spectrum, shown in Fig. 3.

In Fig. 3, the maximum exciting intensity of F* in plasma jet is at the center along the radial direction that decreases gradually with the distance far away from the center position. The active F* atomic intensity distribution changes nearly according to the Gaussian curve in the radial direction, and it matches with the pressure on the workpiece surface shown in Fig. 2

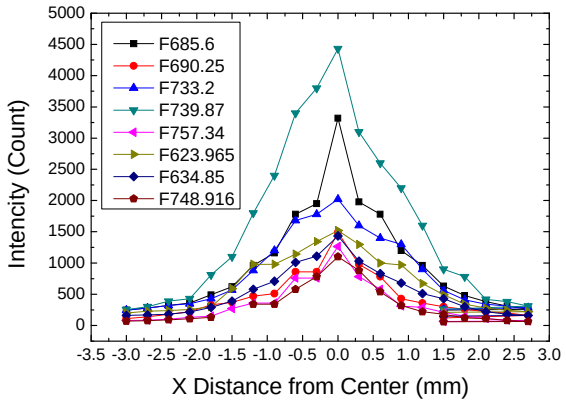

Figure 3. The F intensity distribution along the radial direction.*

3.3 The machining result of the removal function

Fig. 4 shows the surface cross profile of SiO_2 after atmospheric plasma machining. Compared to the simulation results shown in Fig. 2, the jet pressure distribution is proved to be related to the removal volume of the material surface, therefore, jet pressure and namely active species density corresponds to the processing surface.

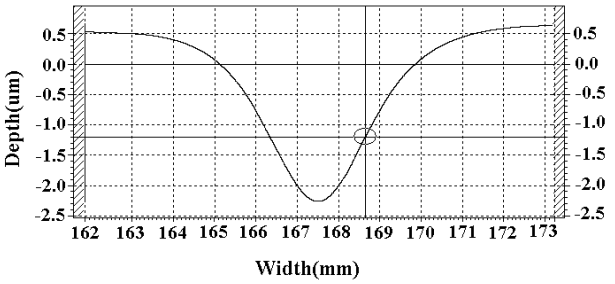

Figure 4. Surface profile of SiO_2 after atmospheric plasma processing.

Thus, we can reach the conclusion that the materials removal rate corresponds to the active radical intensity distribution and the jet pressure on the workpiece surface.

4 Development of the removal function

Two parameters are chosen for the removal function, namely/i.e., etching gas flux L_r, and machining distance between the electrode and the workpiece D. The removal function can be expressed as Equation (4).

$$R(l_r, d) = L(l_r)D(d) \tag{4}$$

From this experiment, using both the surface profile of a workpiece and the processing profile of the plasma jet, a/the Gaussian surface is derived. The expression of the Gaussian surface of unit time is shown as Equation (5).

$$z = ae^{-(x^2+y^2)/c} \tag{5}$$

In this system, the torch may make linear reciprocating displacement versus the workpiece so that at first the removal volume of machining can be obtained indirectly by trench volume and then/ and afterwards the processing parameters a and c of the Gaussian surface can be derived. The removal depth function of the surface can be expressed as the convolution of dwell time and a/the Gaussian surface of unit time processing, as shown in Equation (6).

$$\begin{aligned} h(x,y) &= f(x,y) * g(x,y) \\ &= \iint -ae^{-(u^2+v^2)/c} g(x-u, y-v)dudv \end{aligned} \tag{6}$$

In this system, as the torch may make linear reciprocating displacement to the workpiece, we can make a straight line at y = 0, then $g(x) = k\delta(y)$, where k is dwell time of the unit length, as shown in Equation (7)

$$k = \frac{t}{l} = \frac{1}{V}, \tag{7}$$

where V is the torch speed versus workpiece.

If we substitute Equation (7) into Integral expression, we can achieve Equation (8) with the integral nature of the δ function:

$$\begin{aligned} h(x,y) &= \iint -ae^{-(u^2+v^2)/c} k\delta(y-v)dudv \\ &= \int -ake^{(u^2+y^2)/c} du \end{aligned} \tag{8}$$

The corresponding volume of the Gaussian surface is expressed in Equation (9)

$$\begin{aligned} V_k &= \iint ae^{-(x^2+y^2)/c} dxdy \\ &= a\sqrt{c\pi} \int e^{-y^2/c} dy = ac\pi \end{aligned} \tag{9}$$

Where V_k is known, c is the same as the one in simulated expressions of the section, so the parameter a is shown in Equation (10).

$$a = V_k / c\pi \tag{10}.$$

To determine the removal function that varies with SF_6 flux and machining distance, the following parameters are selected. The supplied power is 200W and the He flux is l SLM, the distance between two electrodes is 1.5mm, and the SF_6 flux is 0, 0.03, 0.06, 0.09, 0.12 SLM, respectively, and the machining distance is 4, 6, 8, 10 mm, respectively.

The experiment result of the variation of parameter a and parameter c with SF_6 flux and machining distance is shown in Fig. 5. Since there are only two independent variables, the relationship of the parameters can be expressed by three-dimensional picture. In Fig. 5, where x, y coordinates represent distance D and SF_6 flow L_r , respectively, and z coordinates represent the Gaussian surface, the parameters a and c correspond to the processing track.

Commercial software is used to fit the expression of the processing parameters a and c, which are shown in Equation (10) and Equation (11), respectively.

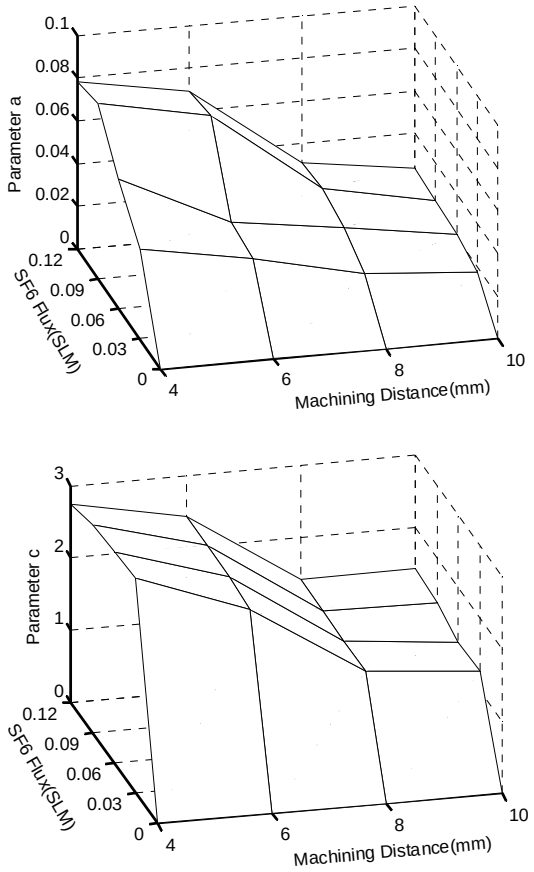

Figure 5. Three-dimensional map of Parameter a (up) and c (below) variation with Machining distance and SF6 flux.

$$a = \frac{p_{a1} + p_{a2} \times D + p_{a3} \times L_r + p_{a4} \times L_r^2 + pa5 L_r^{\ 3}}{1 + p_{a6} \times D + p_{a7} \times D^2 + p_{a8} \times D^3 + p_{a9} \times L_r + p_{a10} \times L_r^2} \quad (10)$$

Here, p_{a1}=-2.3736; p_{a2}=-4.4862E-6; p_{a3}=0.0602; p_{a4}=-0.4246 p_{a5}=1.0813; p_{a6}=-0.4974; p_{a7}=0.0795; p_{a8}=-0.0039; p_{a9}=-0.0529; p_{a10}=0.6676;

$$c = \frac{p_{c1} + p_{c2} \times D + p_{c3} \times D^2 + p_{c4} \times L_r + p_{c5} L_r^{\ 2} + p_{c6} L_r^{\ 3}}{1 + p_{c7} \times D + p_{c8} \times D^2 + p_{c9} \times L_r + p_{c10} \times L_r^{\ 2}} \quad (11)$$

Here, p_{c1}=6.435E-7; p_{c2}=-4.021E-5; p_{c3}=3.472E-5; p_{c4}=12.362; p_{c5}=-146.624; p_{c6}=618.479; p_{c7}=-0.485; p_{c8}=0.077; p_{c9}=-0.004; p_{c10}=0.904;

5 Conclusions

(1) The pressure distribution on the workpiece surface has been simulated according to the jet theory and the active fluorine atomic density distribution has been measured. The results show that the density distribution of active atomic is proportional to the pressure distribution.
(2) Compared to machining results, the removal function profile corresponds to the active fluorine atomics distribution and jet pressure on the workpiece surface.
(3) Based on experimental data of the workpiece profile, the material removal function has been developed by curve fitting, and the reactive gas flux and the distance between the nozzle and the workpiece is calculated by using the parameters of the removal function.

Acknowledgement

This research is supported by the Chinese National Nature Fund, *research into an optic free surface machining technology by atmospheric pressure plasma jet*, the number of which is No. 51175123.

References

[1] Feng, Y., Scholz, L., Lee, D. et al.: *Multi-mode microscopy using diffractive optical elements,* Engineering Review, 31 (2011), 2, 133-139.
[2] Sujová, E.: *Contamination of the working air via metalworking fluids aerosols.* Engineering Review, 32 (2011), 1, 9-15.
[3] Jiao, C.J., Li, S.Y., Xie, X.H. et al.: *Material Removal Property in Ion Figuring Process for Optical Components*, Optical Technique, 34 (2008), 5, 651-654.
[4] Carr, J.W.: *Atmospheric Pressure Plasma Processing for Damage-free Optics and Surfaces,* Engineering Research Development and Technology, 3 (1999), 31-39.
[5] Mori, Y., Yamauchi, K., Yamamura, K. et al.: *Development of plasma chemical vaporization machining*, Review of Scientific Instruments, 71 (2000), 12, 4627-4632.
[6] Takino, H., Yamamura, K., Sano, Y., Mori, Y.: *Shape correction of optical surfaces using plasma chemical vaporization machining with a hemispherical tip electrode,* Applied Optics, 51 (2012), 3, 401-407.
[7] Castelli, M., et al.: *Reactive Atom Plasma for Rapid Figure Correction of Optical Surfaces,* Key Engineering Materials, 496 (2011), 182-187.
[8] Jourdain, R., Castelli, M., Morantz, P., Shore, P.: *Plasma surface figuring of large optical*

components, Proc. SPIE 8430, Optical Micro- and Nanometrology IV, 843011, 2012

[9] Wang, B., Zhao, Q.L., Wang, L.P., Dong, S.: *Application of atmospheric pressure plasma in the ultrasmooth polishing of SiC optics*, Materials Science Forum, 532(2006), 504-507.

[10] Wang, F.J.: *Analysis of computational fluid dynamic*, Beijing: Tsing hua university Press, 2004.

[11] Dean, J.A.: *Analytical Chemisty Handbook*, World Book Publishing Company. 1998.